



Published in final edited form as:

CrystEngComm. 2016 October 14; 18(38): 7269–7275. doi:10.1039/C6CE00659K.

Cooperative elastic switching vs. laser heating in [Fe(phen)₂(NCS)₂] spin-crossover crystals excited by a laser pulse

R. Bertoni^a, M. Lorenc^a, T. Graber^b, R. Henning^b, K. Moffat^b, J.-F. Létard^c, and E. Collet^{a,*}

^a Institut de physique de Rennes, UMR 6251 Université Rennes 1-CNRS, 35042 Rennes, FRANCE.

^b Center for Advanced Radiation Sources, The University of Chicago, Chicago, IL 60637, USA.

^c CNRS, Université de Bordeaux, ICMCB, 87 avenue du Dr. A. Schweitzer, Pessac, 33608 France.

Abstract

Spin-crossover crystals show multi-step responses to femtosecond light excitation. The local molecular photo-switching from low to high spin states occurs on sub-picosecond timescale. It is followed by additional conversion due to elastic (ns) and thermal (μ s) effects. In [Fe(phen)₂(NCS)₂] crystals discussed herein, the thermal switching can be made unobtrusive for the investigation of cooperative elastic switching. We evidence a cooperative transformation induced by lattice expansion through elastic coupling between molecules in the crystal, where up to 3 molecules are transformed per photon.

Introduction

The behaviour of molecules in solid state differs from molecules in solution because of stronger interactions mediated through the lattice. One of the most striking examples is the existence of cooperativity where the responses of elementary components of the material add up in a non-linear fashion. This is especially true for photoinduced phase transitions, where the excitation by a light pulse can abruptly generate cooperative transformations towards a new macroscopic state.¹ Such transformations can be triggered in an ultrafast way where a femtosecond laser pulse impacts the material. During photoinduced phenomena, several microscopic and macroscopic degrees of freedom play their part on significantly different time and length scales. For example, transformations at the molecular scale can be coherently activated^{2,3,4} on the timescale of hundreds of femtosecond. Slower long-range structural reorganizations may induce conductivity or ferroelectricity for example.^{5,6} In addition to localized processes, the entire material can react through lattice deformations and volume expansion occurring on the acoustic time scale^{7,8,9,10}. The understanding of the response of the material at this time scale is of paramount importance because it may stabilize the newly formed photoinduced phase. Here we focus our attention on Spin-

* To whom correspondence should be addressed: eric.collet@univ-rennes1.fr.

crossover (SCO) molecular materials, which are prototypical photoactive materials showing molecular bistability between electronic states differing in physical parameters such as volume, colour, magnetic susceptibility, etc...¹¹ For an Fe(II) system like the [Fe(phen)₂(NCS)₂] single crystal investigated here, the low spin (LS) S=0 state corresponds to a $t_{2g}^6 e_g^0 L^0$ electronic distribution, L referring to ligand orbitals, whereas the high spin (HS) S=2 state corresponds to $t_{2g}^4 e_g^2 L^0$. In the less bonding HS state the <Fe-N> bonding is elongated by $\approx 10\%$ and the molecule swells. The SCO systems are known to be photoswitchable between LS and HS states.¹¹ When induced in the solid state by a femtosecond laser pulse, this process is the initial trigger of a complex out-of-equilibrium dynamics, where different degrees of freedom act at different time and length scales. The qualifying term “molecular materials” unfolds then its genuine meaning: the material response to light stimuli far exceeds the sum of the individual responses of constituting molecules. We have recently demonstrated the possibility of taking advantage of this effect to generate through inter-molecular elastic coupling an elastically-driven cooperative response.¹²

Our previous studies have shown that the out-of-equilibrium transformation of SCO crystals triggered by a fs laser pulse involves three main steps (Fig. 1).¹³⁻¹⁶ The light pulse locally photoswitches molecules from LS to HS via intersystem crossing through metal-to-ligand charge-transfer excitation (MLCT, $t_{2g}^5 e_g^0 L^1$). It was shown by ultrafast techniques that during this photoswitching step, the molecular breathing that accompanies the LS-to-HS photo-conversion occurs in the solid within less than 200 fs whereas vibrational cooling occurs on the ps timescale.^{4,17-21} An initial fraction of HS molecules $X_{HS}^{h\nu}$ is thus photo-generated in the crystal. A second increase of the HS fractions up to X_{HS}^{El} occurs later on the ns timescale. The internal lattice pressure due to HS molecular swelling and the lattice heating induces lattice expansion, driving this additional switching process: the elastic coupling between molecules favours the HS state of higher molecular volume. Because of the global temperature increase of the crystal (≈ 10 s K) a third “thermal” step sets in when the HS population thermally equilibrates to X_{HS}^{Th} with the surrounding hot lattice, typically within 10 μ s. The HS molecular states generated by pulsed laser excitation are transient when induced from the low temperature LS state (typically in the ms range above 100 K).

At very low temperature the lifetime of photoinduced states is much longer and complete conversion can be easily reached by weak *cw* laser excitation.¹¹ Also, a single laser pulse can drive a complete conversion of the material inside thermal hysteresis.^{22,23} As both elastic or thermal effects play their part in the out-of-equilibrium process, it is important to separate these two contributions. Here we investigate the response of photoexcited [Fe(phen)₂(NCS)₂] single crystals by combining time-resolved optical spectroscopy, probing the change of electronic state (HS fraction), and time-resolved x-ray diffraction, probing crystalline lattice change. The first-order nature of the phase transition at thermal equilibrium allows disentangling elastic and thermal effects.

Results and discussion

Thermal transition and the photo-induced steady state

The thermal phase transition of $[\text{Fe}(\text{Phen})_2(\text{NCS})_2]$ crystals was intensively investigated by different spectroscopic and scattering techniques.²⁴⁻²⁸ In this study we used single crystals of typical size $200\mu\text{m}\times 200\mu\text{m}\times 30\mu\text{m}^3$, which undergo a first-order phase transition from purely LS phase below $\approx 180\text{ K}$ to purely HS phase above. The discontinuous change from LS to HS states is accompanied by a large structural reorganization both at the molecular level around the Fe-N₆ core and the macroscopic scale. Fig. 2 shows data reported by Cammarata *et al.*,⁴ which agrees with previous crystallographic studies.^{26,29,30} The average bond length $\langle\text{Fe-N}\rangle$ elongation from 1.97 Å in the LS state to 2.16 Å in the HS state, is characteristic of Fe(II) SCO materials. Through the LIESST effect (Light Induced Electronic Spin State Trapping) discovered in the 80's by Hauser and co-workers,³¹ it is also possible to reach long-lived HS state by weak ^{cw} light excitation at low temperature. Photo-crystallography studies performed at 25 K indicate a global conversion of the crystal after excitation at 660 nm with a ^{cw} laser, associated with an elongation of $\langle\text{Fe-N}\rangle$ up to $\approx 2.16\text{ Å}$ and confirming previous studies on the same compound after excitation at 647 nm.²⁶ An important feature of the LIESST phenomenon is that its quantum efficiency is close to 1, i.e. almost every absorbed photon switches a molecule from LS to HS state.

From the macroscopic point of view, the increase of molecular volume between LS and HS states induces an important lattice expansion, both during the thermal and the photoinduced LS to HS states conversions (Fig. 2).^{4,9,12,17} This can be seen in the discontinuous evolution of the lattice unit cell volume. Figure 3 shows the evolution of the intermolecular distance due to molecular swelling between LS and HS states. In addition to structural changes, another consequence of the change of electronic state during the spin state transition is the change of optical properties. The HS and LS states have different absorption bands due to electronic and structural reorganizations.⁴⁻²¹ This provides a spectroscopic probe of the spin state switching, often used to characterise SCO phenomena.¹¹ Here we monitor the thermal transition in $[\text{Fe}(\text{Phen})_2(\text{NCS})_2]$ single crystals through optical transmission measurements (Fig. 2b) at 950 nm. In this spectral zone, the optical transmission decreases in the HS state of higher optical density than the LS one. The photoexcitation of purely LS crystals by a femtosecond laser pulse into the MLCT band (in the 640-660 nm range) efficiently switches molecules from LS to HS states.^{4,21} The time-resolved optical experiments developed at the *Institut de Physique de Rennes* allow monitoring the optical transmission change after femtosecond photoexcitation, continually from 100 fs to ms, and thereby covering the entire timescale of non-equilibrium dynamics. The time-resolved optical transmission change at a probing wavelength of 950 nm is then scaled in terms of HS fraction X_{HS} . In addition, for investigating the role of lattice expansion in the process, we also performed time-resolved x-ray diffraction studies at the BioCARS beamline³² at the Advanced Photon Source, Argonne National Laboratory (see experimental section).

Response of a single crystal impacted by a femtosecond laser flash

We photoexcited $\approx 25\mu\text{m}$ thick $[\text{Fe}(\text{Phen})_2(\text{NCS})_2]$ single crystals in the tail of the LS MLCT band with a 650 nm light pulse. The penetration depth at this wavelength is on the

order of the thickness of a single crystal. The evolution of the HS fraction X_{HS} after fs laser excitation in the LS phase at 140 K, measured by optical spectroscopy, is shown in Fig. 4 for different excitation densities. The experiment is conducted 40 K below the phase transition to avoid any residual thermal effect and to allow the complete recovery of the LS phase within 1 ms. Our experimental data clearly show a sequence of three steps, similar to the ones already reported in Fe(III) spin-crossover crystals and summarized in Figure 1.¹²⁻¹⁶ First, the absorption of light at the molecular level locally photo-switches a small fraction X_{HS}^{hv} of molecules (typically 2% here) from LS to HS states. We have thoroughly investigated this process in $[\text{Fe}(\text{Phen})_2(\text{NCS})_2]$ crystals with femtosecond optical and x-ray spectroscopies^{4,21} and established that it occurs via ultrafast intersystem crossing. This process involves local coherent structural dynamics and is accompanied by a molecular swelling within 200 fs. X-ray diffraction experiments (Figure 5), performed at 140 K for an excitation density of $20 \mu\text{J}/\text{mm}^2$, reveal that during this initial photoswitching process at the molecular level, the lattice has no time to expand. Indeed the values of the unit cell parameters remain constant up to the ns time scale. The lattice expansion is observed only after a few ns, and occurs concomitantly with a second increase of the HS fraction, reaching X_{HS}^{El} after ≈ 20 ns (Figure 4). The microscopic crystal expansion results from the establishment of a mechanical equilibrium within the crystal: the photoswitched molecules of higher volume exert a negative (or internal) pressure on the lattice, thus causing its expansion. Such effect stems from elastic properities and is responsible for the self-amplified molecular transformation, as recently demonstrated both in experiment and theory.¹² It should be underlined that the cell volume expansion is limited by the propagation of strain waves through the sample. Given the typical acoustic wave velocity ($\sim 2000 \text{ m}\cdot\text{s}^{-1}$) in these materials and the anisotropic shape of the crystals used (lozenge plate) the expansion occurs faster on the short crystal dimension ($\approx 25 \mu\text{m}$ along the c axis) than on the long dimensions ($200\text{-}300 \mu\text{m}$ along the a, b axes). At excitation densities above $40 \mu\text{J}/\text{mm}^2$ there appears a third step in which the HS fraction reaches X_{HS}^{Th} on the $10 \mu\text{s}$ regime (Figure 4).

This effect is associated with the thermal population of the HS state, due to equilibration of the SCO molecules with the hot crystalline lattice, as the absorbed photon energy is converted to heat. As the HS state is more and more populated, the lattice expansion increases anew. The response on the photo, elastic and thermal steps to different excitation densities (expressed in number of incident photon per 100 molecules) is shown in Fig. 4b. The photoswitched fraction X_{HS}^{hv} depends linearly on the laser fluence. By comparing the number of incident photons per molecules in the pump laser pulse with the fractions of photo-switched molecules, we estimate that essentially every photon switches one molecule.

This confirms the quantum efficiency close to unity observed in SCO solids.^{4,12} The photo-response on the elastic step is between 2.5 and 3 times larger than on the photoswitching step. A linear fit of the fraction of HS molecules on the elastic step with the number of incident photons indicates that in average 1 photon transforms ≈ 2.66 molecules (green line in Fig. 4b).

The photoresponse on the thermal step shows a non-linear response and strongly increases with excitation density. To unambiguously assign the last step to thermal effects, we performed similar optical spectroscopy experiments at 140 K and 160 K with an excitation

density fixed at $30 \mu\text{J}/\text{mm}^2$ (Figure 6). At 140 K only the photoswitching and elastic steps are observed resulting in a two-step response in X_{HS} . At 160 K the last thermal step is now observed and characterized by a higher HS population in the μs domain. It is accompanied by a weak lattice expansion in the $100 \mu\text{s}$ regime observed at 160 K under the same $30 \mu\text{J}/\text{mm}^2$ excitation density (orange circle, Fig. 5). The $\approx 2 \text{ \AA}^3$ volume expansion after the thermal step, with respect to the equilibrium values at negative delays, can be compared to the thermal expansion observed at thermal equilibrium. As shown in figure 5, before laser excitation the volume increase between 140 K and 160 K is $\approx 2 \text{ \AA}^3$ (from ≈ 2206 to $\approx 2208 \text{ \AA}^3$). It is therefore reasonable to estimate from the $\approx 2 \text{ \AA}^3$ volume expansion at $100 \mu\text{s}$ delay, that $30 \mu\text{J}/\text{mm}^2$ excitation density generates a ≈ 20 K laser heating. This means that in the time domain the lattice temperature approaches 180 K i.e. the thermal phase transition temperature. It explains the significant thermal population observed at 160 K and for $30 \mu\text{J}/\text{mm}^2$. In contrast photoexcitation at 140 K with the same (Fig. 6) or lower (Fig. 4 & 5) laser fluence is not enough to populate the HS state thermally because of the first-order nature of the phase transition, as the HS fraction changes discontinuously from 0 to 1 around 180 K.

In Figure 6, which compares the photo-reponse after identical laser excitations at 160 and 140 K, it appears that up to $1 \mu\text{s}$ the two curves are identical within the experimental accuracy. At 140 K, the HS molecules converted after the elastic step return to the LS ground state within 1 ms and no further increase of the HS fraction is observed. At 160 K, a significant thermal population occurs on the $10\text{-}100 \mu\text{s}$ scale. The difference (top panel, black triangle, Fig. 6) between the photoexcitation at 160 K and 140 K reveals only the thermal population of HS and demonstrates that this process occurs in the μs -ms regime. The experiment performed at 140 K for different laser fluence also confirms the thermal nature of the μs conversion (Fig. 4). For excitation density below $30 \mu\text{J}/\text{mm}^2$ there is no thermal effect because the temperature jump does not bring the system close enough to the phase transition to populate the HS state. Higher excitation densities induce a larger heating effect. For example at $60 \mu\text{J}/\text{mm}^2$ an almost 40 K temperature jump occurs, if we assume a linear dependence of the temperature jump with the deposited energy on the system. This is enough to bring the system close to the phase transition and populate the HS state thermally. This result is different from previous studies on weakly cooperative Fe(III) SCO materials,^{9,10,17} for which thermal conversion is detected because unlike in a first-order transition, the crossover spans non-critically a broad temperature range. In the present case, it is possible to avoid thermal population when the experiment is performed at a low temperature, or with a low excitation density.

Conclusions

In the out-of-equilibrium process following femtosecond laser excitation of SCO single crystals, three main steps were identified, with characteristic timescales: photo-switching (ps), elastic switching (ns) and thermal switching (μs). One extraordinary aspect of such multiscale response of the material is that it involves different physical processes: from quantum physics and intersystem crossing during the photo-switching step, mechanics during the elastic step and thermodynamics during the thermal step. Our study of $[\text{Fe}(\text{II}) (\text{Phen})_2(\text{NCS})_2]$ SCO material corroborates the previous findings and shows the universality

of this picture in SCO materials. The combination of time-resolved x-ray diffraction and optical spectroscopy reveals clearly the thermal nature of the last step, which can be avoided with appropriate excitation density or initial temperature. In this cooperative SCO material we observe a self-amplified response during the elastic step after excitation of a purely LS state where up to 3 molecules are transformed per photon. Compared to isolated photoactive molecules, with a quantum efficiency attaining at best unity, these results show that mechanical forces induced by absorption of light can induce cooperative switching in volume-changing materials and surpass the single molecule limits. Our previous studies on Fe(III) systems¹² evidenced that the elastic response appears only above a threshold excitation density. It is not the case here as the elastic response varies linearly with excitation density (Fig. 4b). This difference may be attributed to the larger molecular deformation in the Fe(II) systems, where the Fe-ligand distance elongates by ≈ 0.2 Å, whereas for Fe(III) it does only by ≈ 0.15 Å. The energy cost or the elastic coupling is therefore larger as underlined by the first-order character of the phase transition of this compound, compared to the more gradual conversion in Fe(III) systems studied previously. This cooperativity may favor local clustering around photo-switched molecules, resulting in a more linear response. This point will be investigated in future with the mechano-elastic model applied to rationalize this complex out-of-equilibrium transformation at the material scale.¹²

Experimental methods

Time-resolved x-ray diffraction and optical transmission measurements were performed on single crystals, with typical dimensions of $(250\pm 50)\times(200\pm 50)\times(30\pm 5)$ μm^3 . The laser was propagating along the 30 μm thickness corresponding to the crystalline axis c . The single crystals were mounted in nitrogen-flow cryostreams. The optical pump-probe studies were performed at the *Institut de Physique de Rennes* with the experimental setup described in detail in ref. 9. Single crystals were excited with a 80 fs laser flash and their optical transmission was probed by a delayed 80 fs laser probe. The delay between pump and probe was controlled by combining a mechanical translation stage to adjust the optical path difference for sub-ns measurements with an electronic synchronization of the pump and probe amplifiers for measurements in the ns to ms time domain. The experiments were performed with 500 Hz laser pump repetition rate, set to 650 nm on the MLCT band where it efficiently induces LS-to-HS conversion of the $[\text{Fe}(\text{phen})_2(\text{NCS})_2]$ crystal. The probe was set to 950 nm to monitor the LS-to-HS photoswitching dynamics through the variation of optical transmission, and from which X_{HS} was extracted (see also ref. 14 and 21). Time-resolved x-ray diffraction experiments were performed at the BioCARS beamline at the APS synchrotron.³² Single crystals were excited with a ps laser flash centered around 650 nm. Single x-ray pulses (15 keV) were selected by a fast chopper for probing the crystal at different delays, with a 40 Hz repetition rate. The ≈ 70 ps time resolution is limited by the x-ray pulses duration. Partial data were collected in transmission geometry at different pump-probe delays using a single sample rotation axis and the unit cell parameters were obtained from diffraction images with CrysAlis software.³³ The crystallographic data presented in Fig. 2 & 3 were obtained at the *Institut de Physique de Rennes* (see also ref. 4) on a four-circle Oxford Diffraction Xcalibur 3 diffractometer (MoK_α radiation). The single crystals were

mounted in an Oxford Cryosystems nitrogen-flow cryostat for experiments above 78 K and in an Oxford Diffraction Helijet cryostat for measurements at 25 K, where a 660 nm laser diode was used for photoexcitation.

Acknowledgements

This work was supported by the CNRS, the Institut Universitaire de France, Rennes Métropole, the ANR (ANR-13-BS04-0002) and Europe (FEDER). K.M., R.H., T.G. and E.C. thank the University of Chicago for funding through the “France and Chicago Collaborating in the Sciences” (FACCTS) program. The BioCARS facility is supported in part by the Department of Energy (DE-AC02-06CH11357) and in part by the National Institutes of Health grant GM111072 to K.M.. The time-resolved set-up at BioCARS was funded in part through a collaboration with Philip Anfinrud (NIH/NIDDK).

References

1. Nasu, K. Photoinduced Phase Transitions. World Scientific; 2004.
2. Ishikawa T, Hayes SA, Keskin S, Corthey G, Hada M, Pichugin K, Marx A, Hirscht J, Shionuma K, Onda K, Okimoto Y, Koshihara S, Yamamoto T, Hengbo C, Nomura M, Oshima Y, Abdel-Jawad M, Kato R, Miller RJD. *Science*. 2015; 350:1501–1505. [PubMed: 26680192]
3. Johnson SL, Beaud P, Möhr-Vorobeva E, Caviezel A, Ingold G, Milne CJ. *Phys. Rev. B*. 2013; 87:054301.
4. Cammarata M, Bertoni R, Lorenc M, Cailleau H, Di Matteo S, Mauriac C, Matar SF, Lemke H, Chollet M, Ravy S, Laulhé C, Létard J-F, Collet E. *Phys. Rev. Lett*. 2014; 113:227402. [PubMed: 25494090]
5. Gao M, Lu C, Jean-Ruel H, Liu LC, Marx A, Onda K, Koshihara S, Nakano Y, Shao X, Hiramatsu T, Saito G, Yamochi H, Cooney RR, Moriena G, Sciaini G, Miller RJD. *Nature*. 2013; 496:343–346. [PubMed: 23598343]
6. Collet E, Lemée-Cailleau M-H, Buron-Le Cointe M, Cailleau H, Wulff M, Luty T, Koshihara S, Meyer M, Toupet L, Rabiller P, Techert S. *Science*. 2003; 300:612–615. [PubMed: 12714737]
7. Kalantar DH, Belak JF, Collins GW, Colvin JD, Davies HM, Eggert JH, Germann TC, Hawreliak J, Holian BL, Kadau K, Lomdahl PS, Lorenzana HE, Meyers MA, Rosolankova K, Schneider MS, Sheppard J, Stölken JS, Wark JS. *Phys. Rev. Lett*. 2005; 95:075502. [PubMed: 16196791]
8. Lejman M, Vaudel G, Infante IC, Gemeiner P, Gusev VE, Dkhil B, Ruello P. *Nature com*. 2014; 5:4301.
9. Lorenc M, Balde C, Kaszub W, Tissot A, Moisan N, Servol M, Buron-Le Cointe M, Cailleau H, Chasle P, Czarnecki P, Boillot M-L, Collet E. *Phys. Rev. B*. 2012; 85:054302.
10. Collet E, Moisan N, Baldé C, Bertoni R, Trzop E, Laulhé C, Lorenc M, Servol M, Cailleau H, Tissot A, Boillot M-L, Graber T, Henning R, Coppens P, Buron-Le Cointe M. *Phys. Chem. Chem. Phys*. 2012; 14:6192–6199. [PubMed: 22294040]
11. Halcrow, M., editor. Spin-crossover materials. Wiley; West Sussex: 2013. ISBN 9781119998679
12. Bertoni R, Lorenc M, Cailleau H, Tissot A, Laisney J, Boillot M-L, Stoleriu L, Stancu A, Enachescu C, Collet E. *Nature Mater*. 2016 DOI: 10.1038/NMAT4606.
13. Lorenc M, Hébert J, Moisan N, Trzop E, Servol M, Buron-Le Cointe M, Cailleau H, Boillot ML, Pontecorvo E, Wulff M, Koshihara S, Collet E. *Phys. Rev. Lett*. 2009; 103:028301. [PubMed: 19659251]
14. Cailleau H, Lorenc M, Guérin L, Servol M, Collet E, Buron-Le Cointe M. *Acta Cryst. A*. 2010; 66:189. [PubMed: 20164642]
15. Collet E, Lorenc M, Cammarata M, Guérin L, Servol M, Tissot A, Boillot ML, Cailleau H, Buron-Le Cointe M. *Chem. Eur. J*. 2012; 18:2051. [PubMed: 22246788]
16. Marino A, Buron-Le Cointe M, Lorenc M, Toupet L, Henning R, DiChiara AD, Moffat K, Brufel N, Collet E. *Faraday Discuss*. 2015; 177:363–379. [PubMed: 25627455]
17. Bertoni R, Lorenc M, Tissot A, Boillot M-L, Collet E. *Coord. Chem. Rev*. 2015:282–238. 66–76.

18. Bertoni R, Lorenc M, Tissot A, Servol M, Boillot M-L, Collet E. *Ang. Chem. Int. Ed.* 2012; 51:7485–7489.
19. Marino A, Chakraborty P, Servol M, Lorenc M, Collet E, Hauser A. *Ang. Chem. Int. Ed.* 2014; 53:3863–3867.
20. Bertoni R, Lorenc M, Laisney J, Tissot A, Moréac A, Matar SF, Boillot ML, Collet E. *J. Mat. Chem. C.* 2015; 3:7792–7801.
21. Bertoni R, Cammarata M, Lorenc M, Matar S, Létard JF, Lemke H, Collet E. *Acc. Chem. Res.* 2015; 48:774–781. [PubMed: 25705921]
22. Collet E, Henry L, Piñeiro-López L, Toupet L, Real JA. *Current Inorganic Chemistry.* 2016; 6:61–66.
23. Cobo S, Ostrovskii D, Bonhommeau S, Vendier L, Molnár G, Salmon L, Tanaka K, Bousseksou A. *J. Am. Chem. Soc.* 2008; 130:9019. [PubMed: 18570417]
24. König E, Madeja K. *Inorg. Chem.* 1967; 6:48.
25. Müller EW, Spiering H, Gütlich P. *Chem. Phys. Lett.* 1982; 93:567.
26. Marchivie M, Guionneau P, Howard JAK, Chastanet G, Létard JF, Goeta AE, hasseau DC. *J. Am. Chem. Soc.* 2002; 124:194–195. [PubMed: 11782170]
27. Briois V, Cartier dit Moulin Ch. Sainctavit Ph. Brouder Ch. Flank AM. *J. Am. Chem. Soc.* 1995; 117:1019–1026.
28. Baldé C, Desplanches C, Wattiaux A, Guionneau P, Gütlich P, Létard JF. *Dalton Trans.* 2008:2702–2707. [PubMed: 18688401]
29. Gallois B, Real JA, Hauw C, Zarembowitch J. Structural Changes Associated with the Spin Transition in Fe(phen)₂(NCS)₂: A Single-Crystal X-ray Investigation. *Inorg. Chem.* 1990; 29:1152–1158.
30. Granier T, Gallois B, Gaultier J, Real JA, Zarembowitch J. High-Pressure Single-Crystal X-ray Diffraction Study of Two Spin-Crossover Iron(II) Complexes: Fe(Phen)₂(NCS)₂ and Fe(Btz)₂(NCS)₂. *Inorg. Chem.* 1993; 32:5305–5312.
31. Decurtins S, Gütlich P, Köhler CP, Spiering H, Hauser A. *Chem. Phys. Lett.* 1984; 105:1.
32. Graber T, Anfinrud P, Brewer H, Chen Y-S, Cho H-S, Dashdorj N, Henning RW, Kosheleva I, Macha G, Meron M, Pahl R, Ren Z, Ruan S, Schotte F, Šrajer V, Viccaro PJ, Westferro F, Moffat K. *J. Synchrotron Rad.* 2011; 18:658–670.
33. CrysAlis, RED. Version 1.171.26. Oxford Diffraction Ltd; Abingdon, Oxfordshire, England:

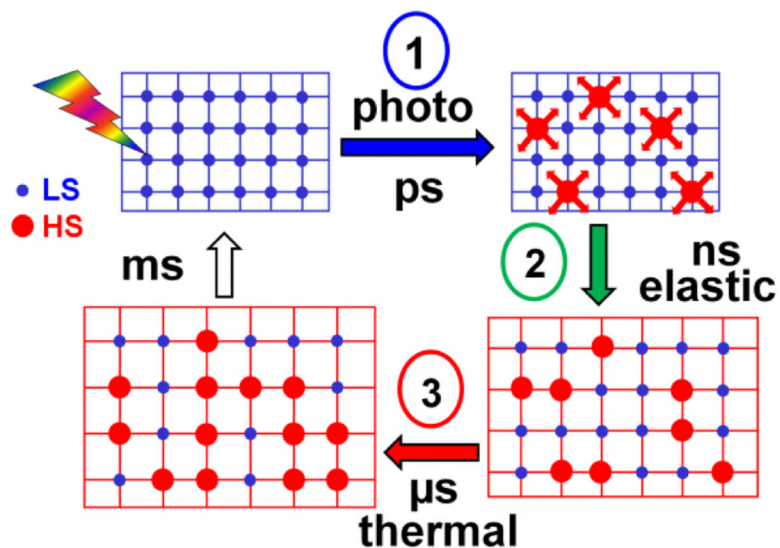


Figure 1. Schematic drawing of the out-of-equilibrium dynamics in SCO crystals. The laser pulse locally photo-switches molecules from LS (blue) to HS (red) states within less than 1 ps (step 1). The molecular swelling and lattice heating induce lattice expansion driving cooperative elastic switching in the ns time window (step 2). The HS state is then thermally populated (μ s) and accompanied by another crystal expansion (step 3).

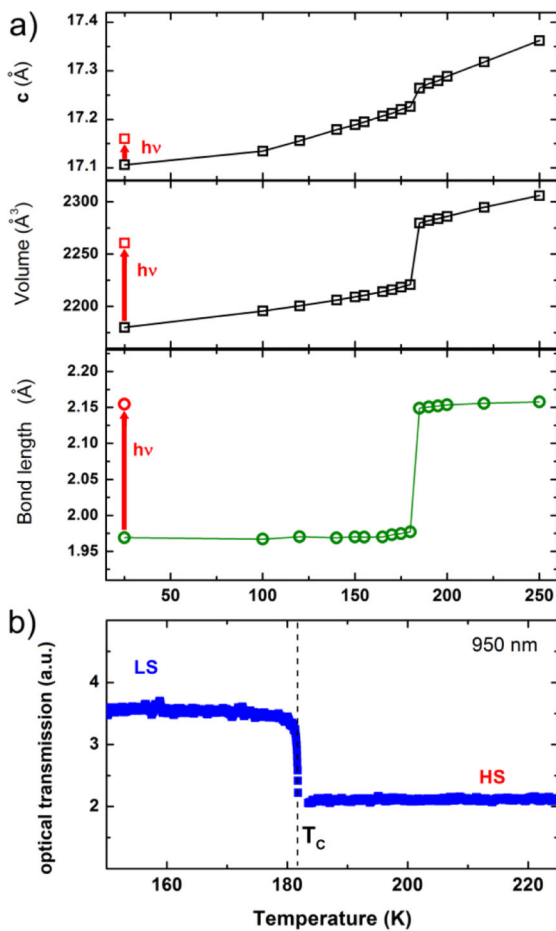


Figure 2. Fingerprints of the conversion between LS and HS states. a) Temperature dependence of the lattice parameter c , the volume V and the $\langle\text{Fe-N}\rangle$ bond length. At 25 K the photoinduced HS state is reached by excitation around 650–660 nm. b) Optical transmission at 950 nm.

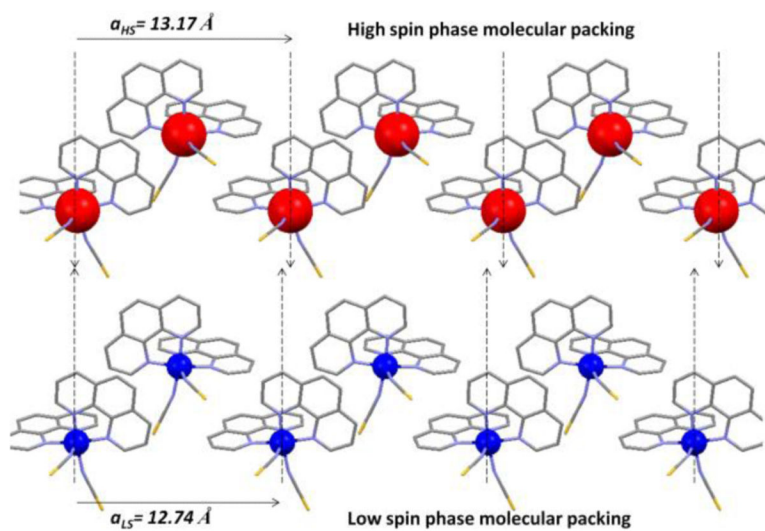


Figure 3. The molecular swelling between LS and HS states induces lattice expansion, shown in along the a crystalline axis.

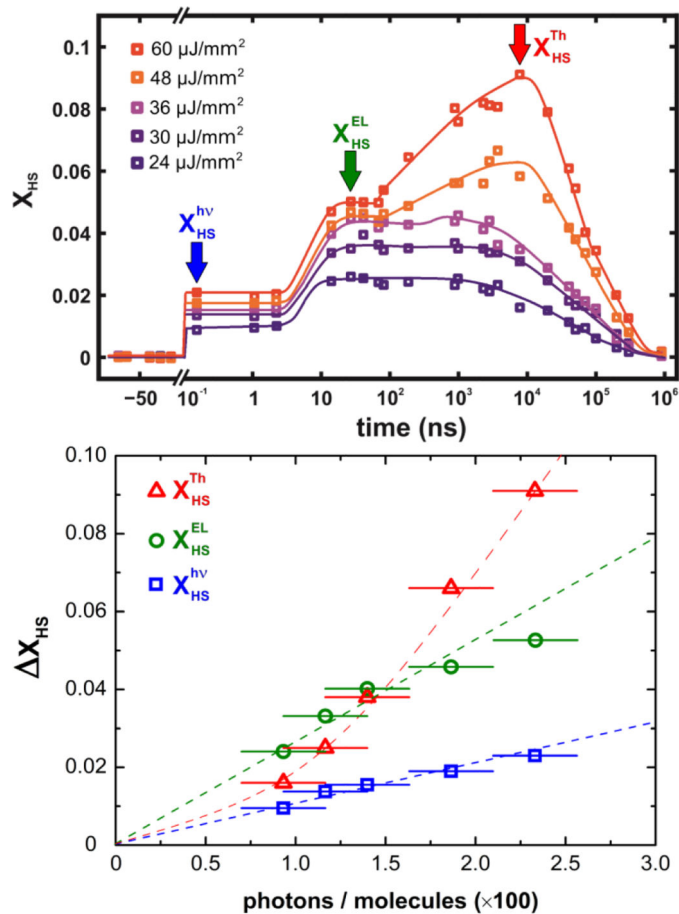


Figure 4.

a) Response to femtosecond laser excitation of LS $[\text{Fe}(\text{Phen})_2(\text{NCS})_2]$ at 140 K for different excitation densities “hv”, “El” and “Th” denote respectively the photoinduced, elastic and thermal steps. b) Evolution of X_{HS}^{hv} (measured at 10 ps) scaling with the number of incident photon per 100 molecules. On the photo-switching step ≈ 1 molecule is transformed per photon, whereas on the elastic step (X_{HS}^{EL}) ≈ 2.5 -3 molecules are transformed per photon. Heating effect appears at high excitation density (close to sample damage).

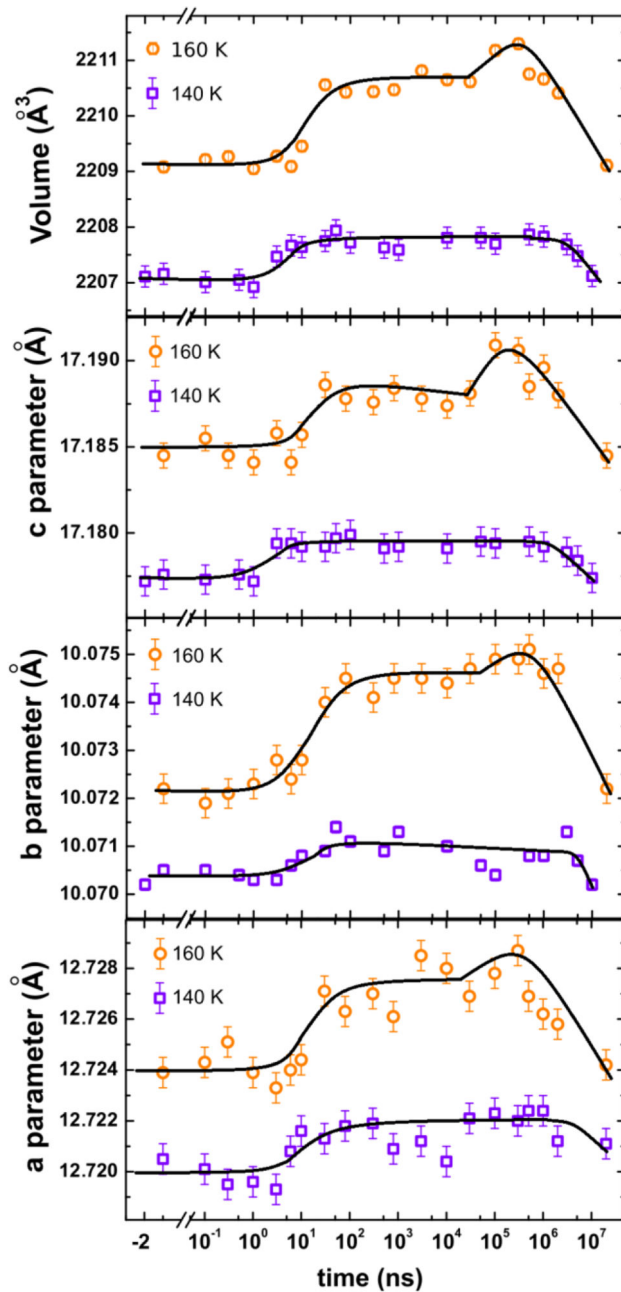


Figure 5.
a) Lattice response to femtosecond laser excitation of LS [Fe(Phen)₂(NCS)₂] at 140 K for an excitation density of 20 $\mu\text{J}/\text{mm}^2$ and at 160 K for an excitation density of 30 $\mu\text{J}/\text{mm}^2$.

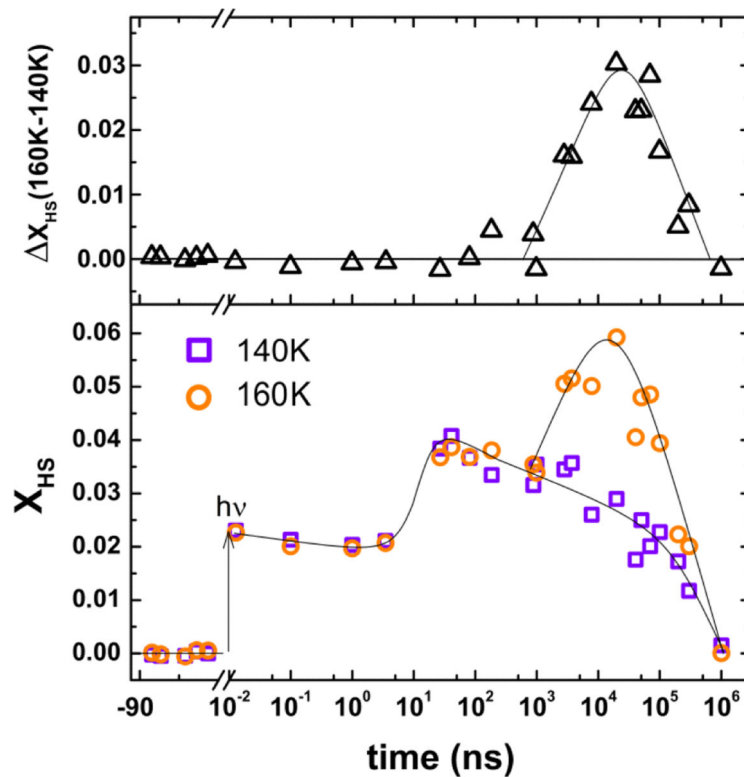


Figure 6. Evolution of the HS fraction X_{HS} after femtosecond laser excitation of LS $[\text{Fe}(\text{Phen})_2(\text{NCS})_2]$ at 140 and 160 K for $30 \mu\text{J}/\text{mm}^2$ excitation density.